Reliable and Low-Latency Communications for Critical Infrastructures Utilizing Wireless Mesh Networks

Ritayan Biswas*, Joonas Säe*, Juho Pirskanen†, and Jukka Lempiäinen*

*Faculty of Information Technology and Communication Sciences (ITC), Tampere University, 33720 Tampere, Finland
Email: {ritayan.biswas, joonas.sae, jukka.lempiainen}@tuni.fi
†Wirepas Ltd., 33270 Tampere, Finland.
Email: {juho.pirskanen}@wirepas.com

Abstract—The purpose of this paper is to evaluate the applicability of wireless mesh networks as a suitable alternative to traditional mobile networks for the monitoring and protection of critical infrastructures. Present-day mobile networks have to handle a large amount of data due to the increase in the need for mobile broadband and the number of users. Therefore, monitoring critical infrastructures exerts an additional load on the existing networks. Thus, the applicability of wireless mesh networks (operating at independent frequency bands) is investigated to determine if they are capable of protecting and monitoring critical infrastructures such as smart grids. The reliability and latency of optimally tuned wireless mesh networks free of other network traffic are studied with the help of simulations based on the DECT-2020 NR standard. It is observed that reliable communications can be realized, however, the end-to-end latency of the network increases with the number of hops and re-transmissions. The user plane latency varies between 10.55 ms to 25.07 ms over five hops and between 15.55 ms to 38.78 ms over eight hops based on the size of the packet. Furthermore, there is a 1.2 to 2 times increment in the latency with each re-transmission. Therefore, a trade-off is necessary to achieve ultra-reliable low-latency communications utilizing wireless mesh networks for monitoring and protection of critical infrastructures.

Index Terms—Critical infrastructure, wireless mesh networks, low-latency, reliable communications, URLLC

I. INTRODUCTION

Critical infrastructures are the fundamental building blocks of modern society. A few infrastructures that are of considerable importance are energy, water, healthcare, communications, banking, and finance to name a few. The smooth operation and proper functionality of these infrastructures can be ensured by preventing significant outage times.

In general, the outage of certain critical infrastructures can be catastrophic if not handled in a timely fashion. Typically, mobile radio systems such as terrestrial trunked radio (TETRA) and Tetrapol in Europe and Project 25 (P25) in Northern America were utilized to relay outage information to different operators [1]. The trend of utilizing commercial mobile networks has been accentuated by the requirement to support state-of-the-art modern applications, smart devices, and the need for high data rates for certain use cases. It is envisioned that long-term evolution (LTE) and 5G networks can support such implementations based on different specifications. 3GPP incorporated mission-critical push-to-talk (MCPTT) for critical communications in LTE Release 13 [2].

The purpose of this article is to evaluate the applicability of wireless mesh networks for monitoring and protection of critical infrastructures as an alternative to traditional commercial mobile networks for communicating outage information of critical infrastructures such as smart grids. The coverage and latency of mesh networks are studied based on the DECT-2020 new radio (DECT-2020 NR) standard [3]–[7]. The simulations are carried out on a smart grid in a rural environment where a line-of-sight (LOS) connection is generally available for each hop. The effect of multiple hops and re-transmissions on the reliability and latency of the system is studied utilizing simulations.

II. THEORY

A. Critical Infrastructures

Fundamental infrastructures provide a backbone to modern society, and the working of these underlying foundation blocks enables the smooth and seamless operation of communities in different parts of the world today. The essential components among a variety of supporting foundation blocks are classified as critical infrastructures. Level 1 infrastructures such as electricity networks, and mobile networks are categorized as the most significant and their orderly functioning is of utmost importance in the event of a disaster or disturbance scenario.

Disasters occur under unforeseen circumstances and are caused due to natural or weather-related anomalies such as cyclones, earthquakes, floods, and wildfires. Furthermore, manmade disturbance scenarios can occur due to war, terrorist or cyber-attacks, and accidents. The ramifications of these disaster and disturbance scenarios are calamitous, and they prohibit the orderly utilization of critical infrastructures. The outages can have devastating effects, and governments utilize a lot of resources to minimize the outage time of these critical infrastructures.

Electrical networks are fundamentally critical infrastructures, as electricity is required to perform the majority of

activities in modern society. Traditional electricity networks consist of generation, transmission, and distribution to end users. The transmission and distribution of electricity are particularly crucial because outages can greatly affect the end users. However, state-of-the-art electricity networks or, smart grids can determine the direction in which the distribution occurs based on the requirement. Additionally, smart grids support a few advanced features, such as advanced monitoring and metering of the network [8]. Furthermore, to aid and minimize the time of the restoration process, remote-controlled switches are utilized [9], [10]. These switches and many other sections of the electrical networks utilize mobile networks to establish a connection. The authors of [11] recommend ensuring power supply to mobile network base stations as an essential method to deal with significant outages of these critical infrastructures.

B. DECT-2020 New Radio

DECT-2020 NR is a set of guidelines proposed by the international telecommunications union (ITU) as an unlicensed, non-cellular 5G radio standard. The DECT-2020 NR standard operates in the unlicensed 1.9 GHz carrier frequency band and is intended to provide support for IoT technologies for massive machine-type communications (mMTC) [3]. This standard was introduced by the ITU keeping in mind that in some specific application scenarios, failure is not a viable option. These scenarios include but are not restricted to critical infrastructures for communities and a variety of operations in the automation industry. Therefore, utilizing the DECT-2020 NR standard, a standalone self-organizing network may be established that provides highly reliable and low-latency communications for a huge number of nodes or radio devices (RDs) [3]. In DECT-2020 NR, RDs operating in a mesh network are capable of communicating directly with each other to extend the range of communication.

The wireless mesh network is a decentralized communication network where the RDs route traffic via single or multiple hops. The decentralized nature of operation enables the RDs in the mesh network to autonomously select their operating mode and optimize the connection accordingly. The RDs can alternate between high-performance low-latency mode or extremely low-power mode depending on the use case. Additionally, the RDs are capable of transitioning between a transmission node, forwarding node, or destination node based on the nature of the message being communicated [3]. This enables reliable, robust, optimized, and scalable connectivity between different RDs. Furthermore, wireless mesh networks are resilient and reliable because if there is a faulty RD, the rest of the RDs organize themselves to find the best possible route to a gateway [3].

Mesh networks may operate based on different types of network topology depending upon the arrangement of the RDs. Star and point-to-point networks are a special realization of mesh networks. In this architecture, a centralized RD receives the data from the adjacent RD. However, following the DECT-2020 NR standard, the clustered tree mesh is the most optimal
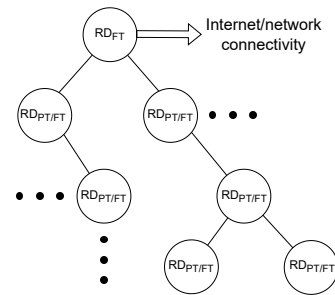

Fig. 1. Network topology of RDs in a clustered tree wireless mesh network.

network topology for uplink data transfer [3]. The data is transmitted to the next hop, and there can be multiple connection points to the external network. A simplified topology of a clustered tree wireless mesh network is shown in Fig. 1. The simulations in this work are performed utilizing RDs organized in the clustered tree wireless mesh network.

The RDs can operate as a fixed termination point (FT), a portable termination point (PT), or both FT and PT modes [3]. Generally, the RDs having a direct connection with the external network operate in the FT mode. Essentially, these RDs regulate the radio resources and enable the RDs operating in the PT mode to connect with them and transfer data to the outside network. An RD operating in the PT mode can start operating in the FT mode after establishing a connection with an RD operating in the FT mode [3]. Therefore, the network can swiftly become scalable as the new RD is capable of handling more RDs.

C. Smart grid protection scenarios

The protection of the smart grid network can be carried out in different ways such as optical fiber (FO), mesh, and cellular (5G) networks. Some of the common protection scenarios of smart grids are illustrated in Fig. 2. The protection scenarios can be classified as:

- Mesh: The mesh-only scenario is shown in Fig. 2a. Communication outside the substation utilizes the mesh network by transferring data from one distribution transformer to another, essentially "jumping" across them, as illustrated by the blue lines in Fig. 2a. The mesh network spans between substations, creating a link between the LAN networks within these substations. This link could serve as an alternative connection for station communication and the supervision of remotely operated separators (depicted as open squares). Typically, the average distance separating distribution substations is approximately 1 km, though some variation may exist. Additionally, substations often feature protective booths to shield against adverse weather and vandalism, with the added capability of providing electricity.
- FO and mesh: This scenario resembles the previous one, but with communication between substations following a more traditional approach through a Wide Area Network (WAN), often implemented using optical fiber (depicted
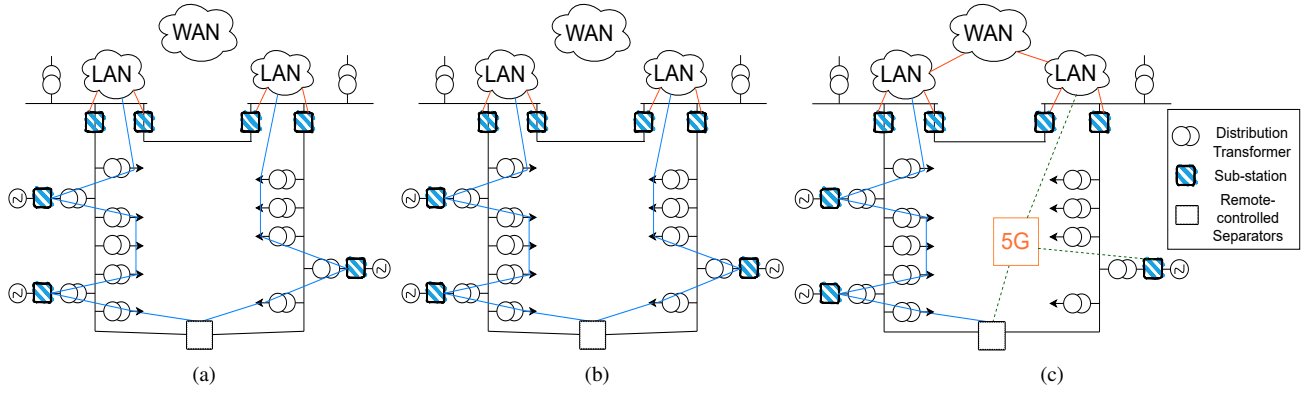
Fig. 2. The different protection scenarios for smart grids. Fig. 2a illustrates the mesh-only protection scenario. In Fig. 2b, the protection scenario where FO and mesh networks are used is shown. Fig. 2c demonstrates the protection scenario using, FO, mesh, and 5G networks.

as red lines). In such cases, the mesh network is extended only as far as necessary, particularly when it comes to Local Out-of-Service (LOM) protection for generators. The conventional SCADA communication for substations and remote-controlled disconnectors is organized via the WAN network using optical fiber, and for remote-controlled disconnectors, it employs technologies like 3G/4G, denoted by the green line. When the configuration of the electrical network changes such that all generators are connected to the same medium voltage output, communication for some generators must have the capability to "route" through the WAN network to another substation and then proceed through the mesh network to reach the generator. This occurs even if the electrical power supply for the generator does not originate from the substation in question.

- FO, mesh, and 5G: This represents a further extension of the previous version. The concept here revolves around the utilization of the 5G network in cases where, for various reasons, implementing a mesh network is either not feasible or becomes cost-prohibitive.

III. SIMULATION SETUP AND PARAMETERS

A. Packet structure

The packet structure includes the synchronization training field (STF), the guard interval (GI), and the data field (DF) [5]. The STF is composed of either 7 or 9 periodic repetitions of the sequence. The transmission of the STF commences at the boundary of the transmission allocation. The GI at the end of the packet helps to avoid an overlap in adjacent TDMA time-slot transmissions. The DF contains the number of OFDM symbols with the corresponding cyclic prefix (CP). The length of the OFDM symbols is dependent on the sub-carrier scaling factor μ. The DF also transmits the demodulation reference signal (DRS), the physical control channel (PCC), and the physical data channel (PDC) [5]. In this work, the calculations for the packet structure are done for $\mu = 1$.

The transmission packet length in terms of OFDM symbols is:

$$N_{\text{symb}}^{\text{PACKET}} = PacketLength \cdot N_{\text{symb}}^{\text{SLOT},\mu}, \tag{1}$$

where the $PacketLength$ is defined based on the packet length type in the physical header and specified based on the number of slots or sub-slots [6].

The DF length in terms of OFDM symbols is expressed as:

$$N_{\text{symb}}^{\text{DF}} = N_{\text{symb}}^{\text{PACKET}} - N_{\text{symb}}^{\text{GI + STF}}, \tag{2}$$

where the value of $N_{\text{symb}}^{\text{GI + STF}}$ is 2 when μ is 1.

The number of DRS resource elements ($N_{\text{re}}^{\text{DRS}}$) for a packet is expressed by,

$$N_{\text{re}}^{\text{DRS}} = N_{\text{TX}}^{\text{eff}} \cdot \frac{N_{\text{OCC}}^{\beta}}{4} \cdot \left\lfloor \frac{N_{\text{symb}}^{\text{PACKET}}}{N_{\text{step}}} \right\rfloor, \tag{3}$$

where $N_{\text{TX}}^{\text{eff}}$ is 1, N_{OCC}^{β} is 56 and N_{step} is 5 as $N_{\text{TX}}^{\text{eff}} \le 2$.

The number of resource elements for the physical data channel ($N_{\text{re}}^{\text{PDC}}$) is computed as:

$$N_{\text{re}}^{\text{PDC}} = N_{\text{symb}}^{\text{DF}} \cdot N_{\text{OCC}}^{\beta} - N_{\text{re}}^{\text{DRS}} - N_{\text{re}}^{\text{PCC}}, \tag{4}$$

where the value of $N_{\text{re}}^{\text{PCC}}$ is 98.

The maximum number of bits that can be carried by the PDC is calculated using Eq. 5,

$$N_{\text{bits}}^{\text{PDC}} = \lfloor N_{\text{SS}} \cdot N_{\text{re}}^{\text{PDC}} \cdot N_{\text{bps}} \cdot R \rfloor, \tag{5}$$

where $N_{\text{SS}} = 1$ and represents the number of parallel spatial streams, N_{bps} the bits per symbol having values of $[2, 4]$, and R the coding rate having values of $[\frac{1}{2}, \frac{3}{4}]$.

Finally, the size of the transport block ($N_{\text{bits}}^{\text{TB}}$) is determined using Eq. 6,

$$N_{\text{bits}}^{\text{TB}} = N_{\text{M}} - (C + 1) \times L, \tag{6}$$

where N_{M} is calculated utilizing Eq. 7, C represents the transport block segmentation parameter and is calculated based on Eq. 8, and L represents the CRC length having a value of 24.

TABLE I
PACKET SIZE (IN BITS) BASED ON MCS. TRANSMISSION DURATION
CORRESPONDS TO THE PACKET SIZE.

Transmission duration $(t_{\text{duration}}, \mu\text{s})$	QPSK (1/2)	QPSK (3/4)	16-QAM (1/2)
208.33	32	56	88
416.67	296	456	616
625.00	552	856	1128
833.33	824	1256	1672
1041.67	1096	1640	2168
1250.00	1352	2024	2680
1458.33	1608	2360	3192
1666.67	1864	2744	3704

$$N_{\text{M}} = \left\lfloor \frac{N_{\text{bits}}^{\text{PDC}}}{M} \right\rfloor \times M, \tag{7}$$

where the value of M is 8 if $N_{\text{bits}}^{\text{PDC}} \leq 512$, 16 if $N_{\text{bits}}^{\text{PDC}} \leq 1024$, 32 if $N_{\text{bits}}^{\text{PDC}} \leq 2048$ otherwise M is 64.

$$C = \left\lceil \frac{N_{\text{M}} - L}{Z} \right\rceil, \tag{8}$$

where Z represents the maximum turbo encoder block size. In this work, the value of Z is considered to be 2048.

If $N_{\text{M}} \leq Z$ then the transport block is unsegmented and Eq. 6 is modified to Eq. 9,

$$N_{\text{bits}}^{\text{TB}} = N_{\text{M}} - L. \tag{9}$$

The size of the data packet (in bits) is calculated utilizing either Eq. 6 or Eq. 9 based on the modulation and coding schemes (MCS) and is summarized in Table I.

B. User plane latency

The user plane latency is computed depending on whether the hybrid automatic repeat request (HARQ) is necessary or not. The utilization of HARQ enables the system to be more robust and reliable. However, the HARQ feedback transmission and the time for the data re-transmission have to be taken into account when HARQ is necessary for the system [7].

The simulations are performed with the sub-carrier scaling factor ($\mu = 1$) and the Fourier transform scaling factor ($\beta = 1$). Based on the DECT-2020 NR frame structure, 5 symbols can be transmitted in one sub-slot, and the time duration is evaluated to be 208.33 microseconds [5]. Therefore, the minimum data packet transmission duration (t_{duration}) from Table I is 208.33 microseconds or 0.208 ms. The t_{duration} of each packet is summarized in Table I.

The symbol alignment time (t_{sym}) is a necessary parameter utilized in the calculation of the user plane latency. The value of t_{sym} is 0.5 times the length of the symbol, which for DECT-2020 NR systems is 0.0416 ms. Therefore, the value of t_{sym} is 0.0208 ms. Additionally, the duration for the data transfer (T_1) is computed taking into account the TX processing delay ($t_{\text{rd\_tx}}$), RX processing delay ($t_{\text{rd\_rx}}$), and the transmission duration (t_{duration}) utilizing Eq. 10,

$$T_1 = t_{\text{rd\_tx}} + t_{\text{duration}} + t_{\text{rd\_rx}}, \tag{10}$$

where the duration of $t_{\text{rd\_tx}}$ is 0.5 ms (for T_1) which is a bit more than the duration of two sub-slots. The value of $t_{\text{rd\_rx}}$ is one sub-slot or 0.2083 ms. The value of $t_{\text{rd\_rx}}$ is the same in the subsequent calculations.

The HARQ transmission duration (T_2) is computed utilizing Eq. 11,

$$T_2 = \max(t_{\text{rd\_tx}}, t_{\text{backoff}}) + t_{\text{HARQ}} + t_{\text{rd\_rx}}, \tag{11}$$

where the t_{backoff} represents the duration of time the system needs to wait before the HARQ transmission can proceed. The duration of the back-off time is set to 0.33 ms. The value of the TX processing delay for T_2 is 0.2083 ms. The same value is utilized for $t_{\text{rd\_tx}}$ in the subsequent calculations. The HARQ duration (t_{HARQ}) is the duration of one sub-slot or 0.2083 ms.

Subsequently, the data re-transmission (T_3) duration is computed utilizing Eq. 12,

$$T_3 = \max(t_{\text{rd\_tx}}, t_{\text{backoff}}) + t_{\text{duration}} + t_{\text{rd\_rx}}, \tag{12}$$

where the duration of t_{backoff} is 0.33 ms. Based on the MCS and the transmission packet size the t_{duration} is computed and the values are summarized in Table I.

The one-way user plane latency without HARQ is calculated by utilizing Eq. 13,

$$T_{\text{UP}} = t_{\text{sym}} + T_1 + t_{\text{ack}}. \tag{13}$$

If data re-transmission is necessary, the user plane latency is computed utilizing Eq. 14,

$$T_{\text{UP}} = t_{\text{sym}} + T_1 + n \times (T_2 + T_3) + t_{\text{ack}}, \tag{14}$$

where the t_{ack} term in Eq. 13 and Eq. 14 represents the duration of the acknowledgement. The duration of t_{ack} is one sub-slot or 0.2083 ms. The number of re-transmissions required is denoted by the parameter n, where $n \geq 0$.

The computation of the user plane latency is performed utilizing parameters that can change and therefore modify the results. Thus, certain assumptions are made to present the results coherently. Firstly, the data packet is not fragmented for transmission. Therefore, once the data transmission begins, the entire packet is transmitted. From Table I, the smallest packet is transmitted over one slot or sub-slot, and the largest packet utilizes 4 slots/8 sub-slots. Secondly, the underlying principle for data transmission is the slotted ALOHA protocol. The randomization is based on the DECT-2020 NR frame structure, where the data transmission can begin at any of the 48 sub-slots. However, it is important to tune the parameters optimally and not wait for too many sub-slots for the data transmission. This ensures there is no additional latency in the system due to the random selection of the sub-slot. Additionally, the data transmission can exceed the frame time (10 ms). Moreover, the messages generated for the protection of critical infrastructures are transmitted over reserved channels (exempt from other

TABLE II
MINIMUM USER PLANE LATENCY WITHOUT AND WITH HARQ BASED ON PACKET SIZE OVER A SINGLE HOP.

Packet size (bits)	32	296	552	824	1096	1352	1608	1864
Without HARQ (ms)	1.35	1.56	1.76	1.97	2.18	2.39	2.59	2.80
HARQ (ms)	3.05	3.47	3.88	4.30	4.71	5.13	5.53	5.95

TABLE III
USER PLANE LATENCY WITHOUT AND WITH HARQ BASED ON PACKET SIZE OVER A SINGLE HOP.

Packet size (bits)	32	296	552	824	1096	1352	1608	1864
Without HARQ (ms)	1.77	1.97	2.18	2.39	2.60	2.81	3.01	3.22
HARQ (ms)	3.88	4.30	4.72	5.13	5.55	5.97	6.37	6.79

TABLE IV
USER PLANE LATENCY WITHOUT AND WITH HARQ BASED ON PACKET SIZE OVER FIVE HOPS.

Packet size (bits)	32	296	552	824	1096	1352	1608	1864
Without HARQ (ms)	5.10	6.14	7.18	8.22	9.26	10.31	11.31	12.36
HARQ (ms)	10.55	12.63	14.71	16.80	18.87	20.97	22.97	25.07

TABLE V
USER PLANE LATENCY WITHOUT AND WITH HARQ BASED ON PACKET SIZE OVER EIGHT HOPS.

Packet size (bits)	32	296	552	824	1096	1352	1608	1864
Without HARQ (ms)	7.60	9.26	10.92	12.60	14.25	15.93	17.53	19.21
HARQ (ms)	15.55	18.87	22.20	25.55	28.86	32.22	35.42	38.78

traffic) to optimize latency and other system parameters. Finally, the MCS utilized in the simulations is QPSK with a coding rate of $1/2$.

IV. RESULTS AND ANALYSIS

The latency for end-to-end communications is computed for different scenarios where single or multiple hops via RDs may be necessary to transmit the data to the gateway for processing. Typically, in practical scenarios, one hop is insufficient as it does not offer a long enough distance to transfer the data to the gateway. Therefore, in this work, the latency for one, five, and eight hops between the first RD and the gateway is computed to provide an accurate estimation of the duration to transmit the data.

The calculation of end-to-end communication latency is performed for various scenarios where data transmission to the gateway requires either a single hop or multiple hops through RDs. In practical situations, a single hop often falls short of covering the necessary distance for data transfer to the gateway. Consequently, in this study, the latency is computed for one, five, and eight hops between the initial RD and the gateway. This comprehensive analysis provides a precise estimate of the time required for data transmission.

The attainable communication range between RDs that have a Line of Sight (LOS) was determined using the Free Space Path Loss (FSPL) equation. It is assumed that the RDs employed for safeguarding and monitoring smart grids enjoy an unobstructed LOS connection with each other, often positioned atop power lines. This positioning ensures that the RDs maintain a direct, obstacle-free LOS connection, bypassing any irregularities related to the terrain.

The path loss value was calculated based on data from [4]. In this calculation, it was considered that the maximum output power of a class I RD is 23 dBm, and the receiver sensitivity, with a bandwidth of 1.728 MHz, is -99.7 dBm. Additionally, an extra margin of approximately 10 dB was factored into the computations. This margin takes into account the added signal propagation loss, which may occur due to factors such as blockage of the Fresnel zone. It was observed that, under these conditions, the achievable one-hop distance between two RDs positioned within LOS is 5.4 km when operating at a carrier frequency of 1.9 GHz.

For each hop, the latency between the two RDs is calculated depending on whether the transmission starts immediately in the first available sub-slot or if the system is configured with a specific back-off duration before transmission can begin. The back-off duration (t_{backoff}), is set to 0.33 ms, which corresponds to a transmission delay of 2 sub-slots. Consequently, in this scenario, data transmission initiates during the third sub-slot.

As a result, the minimum user plane latency (in cases where there is no back-off) for various packet sizes can be found in Table II. Similarly, the user plane latency when factoring in the back-off duration is presented in Table III.

Table II reveals that the packet size indeed influences the duration of transmission. Furthermore, the latency doubles when HARQ transmissions are introduced. This outcome is logical since HARQ transmissions enhance error resilience, albeit at the cost of longer transmission times in comparison to non-HARQ transmissions.

Table III demonstrates that the introduction of a reasonable back-off time leads to an increase in data transmission duration. This occurs because the system must delay data transmission to ensure synchronization between transmitting and receiving RDs. However, the incorporation of a back-off time in such systems is justifiable, and subsequent calculations account for this back-off duration.

In real-world scenarios, multiple RDs play a role in transmitting data to the destination RD or gateway. Table IV provides a summary of the user plane latency for a system with five hops. It's noteworthy that, akin to the single-hop scenario, the packet size has a direct impact on the duration of data transmission. Additionally, it's evident that for a given
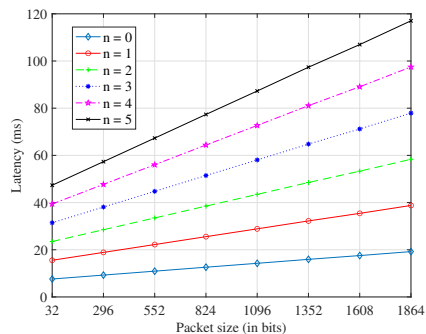
Fig. 3. User plane latency over eight hops as a function of the packet size and the number of re-transmissions (n).

packet size, the transmission duration increases approximately by a factor of around 3.5–4 times when data is transmitted over five hops.

Table V provides a summary of the user plane latency for a system with eight hops, categorized by packet size. Notably, when compared to a single-hop scenario, it's observed that the end-to-end latency increases by a factor ranging from 4 to 5.7 times when data is transmitted over eight hops.

The simulations mentioned were conducted under the assumption of a single re-transmission ($n = 1$). As expected, latency increases as the number of re-transmissions rises. Fig. 3 illustrates the latency, categorized by the number of re-transmissions, for each packet size over eight hops. Notably, for a given packet size, latency doubles during the first re-transmission ($n = 1$). In contrast, for the fifth re-transmission ($n = 5$), the latency increases by approximately 1.2 times compared to the fourth re-transmission ($n = 4$). Thus, the overall end-to-end latency of the system is generally influenced by the number of re-transmissions required to transmit data from the initial RD to the gateway.

Moreover, the URLLC requirement of ETSI specifications states that the target user plane latency in 5G systems is 0.5 ms in uplink and downlink, respectively [12]. Furthermore, for infrequent small packets, 5G systems have a latency of 10 ms for a packet size of 160 bits without HARQ re-transmissions [12]. Therefore, it can be inferred that wireless mesh networks provide similar latency values in comparison to present 5G systems depending on the use case of protection or monitoring of the network.

V. CONCLUSION

The objective of this article was to assess the suitability of wireless mesh networks for protecting and monitoring critical infrastructures like smart grids. This evaluation was conducted by analyzing the end-to-end latency of wireless mesh networks, following the DECT-2020 NR standard. The study revealed that a distance of approximately 5 km could be covered per hop for RDs situated within LOS, which could be valuable in decentralized local communication, particularly in protection scenarios. It was evident that system latency increased with the size of data packets. Additionally, the number of

hops had a substantial impact on end-to-end delay, with latency ranging from approximately 10.55 ms to 25.07 ms for five hops and 15.55 ms to 38.78 ms for eight hops, depending on data packet size. Furthermore, the overall system latency increased by around 1.2 to 2 times with each re-transmission. While re-transmissions enhance system robustness, they introduce delays between packet generation and delivery. To achieve low-latency communications with a 99 % probability, a trade-off must be struck. This can be accomplished by minimizing the number of re-transmissions required to deliver the packet to the gateway. In comparison with 5G systems, wireless mesh networks demonstrated a realistic end-to-end delay for packet delivery. Therefore, it can be concluded that wireless mesh networks possess the capability to effectively contribute to the protection and monitoring of critical infrastructures such as smart grids.

REFERENCES

[1] A. Kumbhar, F. Koohifar, I. Güvenç, and B. Mueller, "A survey on legacy and emerging technologies for public safety communications," *IEEE Communications Surveys and Tutorials*, vol. 19, no. 1, pp. 97–124, 2017.

[2] S. Mukherjee and C. Beard, "A framework for ultra-reliable low latency mission-critical communication," in *2017 Wireless Telecommunications Symposium (WTS)*, 2017, pp. 1–5.

[3] European Telecommunications Standards Institute (ETSI), *ETSI TS 103 636-1 V1.4.1 (2023-01), DECT-2020 New Radio (NR); Part 1: Overview; Release 1*, 01 2023. [Online]. Available: https://www.etsi.org/deliver/etsi_ts/103600_103699/10363601/01.04.01_60/ts_10363601v010401p.pdf

[4] ——, *ETSI TS 103 636-2 V1.4.1 (2023-01), DECT-2020 New Radio (NR); Part 2: Radio reception and transmission requirements; Release 1*, 01 2023. [Online]. Available: https://www.etsi.org/deliver/etsi_ts/103600_103699/10363602/01.04.01_60/ts_10363602v010401p.pdf

[5] ——, *ETSI TS 103 636-3 V1.4.1 (2023-01), DECT-2020 New Radio (NR); Part 3: Physical layer; Release 1*, 01 2023. [Online]. Available: https://www.etsi.org/deliver/etsi_ts/103600_103699/10363603/01.04.01_60/ts_10363603v010401p.pdf

[6] ——, *ETSI TS 103 636-4 V1.4.1 (2023-01), DECT-2020 New Radio (NR); Part 4: MAC layer; Release 1*, 01 2023. [Online]. Available: https://www.etsi.org/deliver/etsi_ts/103600_103699/10363604/01.04.01_60/ts_10363604v010401p.pdf

[7] ——, *ETSI TR 103 810 V1.1.1 (2021-11), ETSI Evaluation Group; Final Evaluation Report on DECT-2020 NR*, 11 2021. [Online]. Available: https://www.etsi.org/deliver/etsi_tr/103800_103899/103810/01.01.01_60/tr_103810v010101p.pdf

[8] CEN/CENELEC/ETSI Joint Working Group on Standards for Smart Grids, *Final report of the CEN/CENELEC/ETSI Joint Working Group on Standards for Smart Grids*, May 2011. [Online]. Available: https://www.etsi.org/images/files/Report_CENCLCETSI_Standards_Smart_Grids.pdf

[9] D. P. Bernardon, V. J. Garcia, M. Sperandio, J. L. Russi, E. F. B. Daza, and L. Comassetto, "Automatic re-establishment of power supply in distribution systems using smart grid concepts," in *2010 IEEE/PES Transmission and Distribution Conference and Exposition: Latin America (T & D-LA)*, 2010, pp. 44–49.

[10] F. Edström and L. Söder, "Impact of remote control failure on power system restoration time," in *2010 IEEE 11th International Conference on Probabilistic Methods Applied to Power Systems*, 2010, pp. 343–347.

[11] S. Horsmanheimo, N. Maskey, L. Tuomimäki, H. Kokkoniemi-Tarkkanen, and P. Savolainen, "Evaluation of interdependencies between mobile communication and electricity distribution networks in fault scenarios," in *2013 IEEE Innovative Smart Grid Technologies-Asia (ISGT Asia)*, 2013, pp. 1–6.

[12] European Telecommunications Standards Institute (ETSI), *ETSI TR 138 913 V14.3.0 (2017-10), 5G; Study on scenarios and requirements for next-generation access technologies (3GPP TR 38.913 version 14.3.0 Release 14)*, 01 2023. [Online]. Available: https://www.etsi.org/deliver/etsi_tr/138900_138999/138913/14.03.00_60/tr_138913v140300p.pdf